Proceedings of the
47th IEEE Conference on Decision and Control
Cancun, Mexico, Dec. 9-11, 2008

Transition Control of Plane Poiseuille Flow - A Spatially Interconnected Model

Saulat S. Chughtai
Institute of Control Systems
Hamburg University of Technology
Hamburg 21073 Germany
Email:saulat.chughtai@tu-harburg.de

Herbert Werner
Institute of Control Systems
Hamburg University of Technology
Hamburg 21073 Germany
Email:herbert.werner@tu-harburg.de

Abstract— **This paper proposes a new mathematical model for the transition control problem in plane Poiseuille flow. Most of the previously proposed models are based on pseudospectral approaches and are valid only for a single spatial wave number. In this work we propose a new model which is based on a finite difference approach in streamwise direction and a spectral approach in wall normal direction. The model obtained is valid for all spatial frequencies and can be used for the synthesis of controllers for flow control problems, using some recently developed ideas for spatially interconnected systems. Since these controllers are designed in physical domain they are simple to implement using MEMS arrays. The model is compared with results obtained with previously proposed models and is found to be in good agreement with them. To illustrate its usefulness, a stabilizing dynamic output feedback controller is designed for a Reynolds number of 6000.**

I. Introduction

In many engineering applications the process of laminar-turbulence transition in plan Poiseuille flow is of particular importance. Laminar flow exhibits less drag and heat transfer, whereas turbulent flow is required for thorough mixing. The use of linear control theory for controlling flow instabilities, which cause the transition, is a fairly new approach. Earlier work related to this field mostly concentrates on superimposing anti-phase modes to cancel sinusoidal disturbances.

The underlying control scheme has an array of sensors which measure stream-wise and span-wise skin friction. The actuators are mounted on the walls which can change the boundary condition on the wall normal component of velocity. A detailed exposition of the problem can be found in [1].

In order to synthesize a controller for flow transition, using modern control approaches, one requires a mathematical model. The dynamical behavior of laminar flow is governed by Navier-stokes equations (NSE). Which are nonlinear coupled partial differential equations. In order to model the transition from laminar to turbulent these are linearized around the laminar flow. If the standard linearized NSE are used, the final state space representation results in a singular system. In order to avoid this singularity, three possible formulations of NSE can be used [2], which are: a velocity-vorticity formulation, a stream wise function formulation and a velocity-pressure formulation. Spectral methods are then used to approximate the dynamics of the system for a particular spatial frequency and time evolution of velocities away from boundaries. This approach is used to model the plane Poiseuille flow transition in [3], [4], [5], [6], [7]. The model so obtained is parameterized with Reynolds number and spatial wave numbers. However, controllers designed on using these models are hard to implement as they work in Fourier domain, which requires online Fourier transformation and inverse Fourier transformation of inputs and outputs.

In this paper we propose a combined pseudospectral and finite difference approach to model the flow transition, where finite difference is used in the direction of flow and Chebyshev basis functions are employed for the wall normal direction. The case presented here is for two dimensional flow only, however, one can easily extend the approach for the three dimensional case also. A similar approach has been proposed in [8]. However, our approach is different in a number of aspects from the model used in [8]. These differences can be summarized as follows:

- The model is based on a velocity-vorticity formulation. There are many advantages in using this formulation, as discussed in [9] and the references therein.
- The model has different inputs and outputs, compared with previously proposed models. Here, each actuator can produce either a blowing or suction effect rather then coupled blowing and suction and the output is not shear force but change in shear force in x-direction.
- The model proposed here is independent of the length of the spatial chain, unlike the model presented in [8], which is only applicable to vibrating ribbon problems. Since in the proposed model the number of states increases by N (number of Chebyshev polynomials used) each time a new element is included in the chain.
- The model presented here can be used to synthesize controllers using efficient techniques like the one presented in [10], [11],[12],[13], thus avoiding the heuristic curve fitting approach , which is required in the model proposed in [8] to reduce the model order.

The paper is organized as follows: In section 2 the NSE and its velocity-vorticity formulation are reviewed. These will be used for modeling the flow transition control problem in section 3. Section 4 presents a comparison of the spatially distributed model obtained here with results from previously

978-1-4244-3124-3/08/$25.00 ©2008 IEEE

presented models. In section 5 the model is used for the synthesis of a full order dynamic output feedback stabilizing controller for a Reynolds number of 6000, which is known to be spatially unstable [3]. In the last section conclusions are drawn and some future directions are presented.

II. NSE FOR FLOW TRANSITION CONTROL

Consider a two-dimensional steady state plane channel flow with maximum velocity U_0 and channel half-width δ as shown in Figure 1.

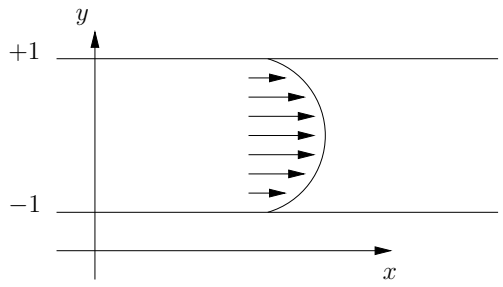

Fig. 1. Plane Poiseuille flow, 2D case

The standard NSE can be linearized by first normalizing all velocities about the centreline velocity U_0 and half height δ. Then, assuming laminar flow, the NSE can be linearized around the mean velocity profile in the streamwise direction (x). For laminar flow the mean velocity profile can be written as $U(y) = 1 - y^2$ on the domain $y \in [-1, 1]$. The equation governing small, incompressible, three-dimensional perturbations $\{u, v, p\}$ are then given by the linearized NSE and the continuity equations,

$$\begin{aligned} \frac{\partial u}{\partial t} + U\frac{\partial}{\partial x}u + \frac{dU}{dy}v &= -\frac{\partial p}{\partial x} + \frac{1}{Re}\Delta u \\ \frac{\partial v}{\partial t} + U\frac{\partial}{\partial x}v &= -\frac{\partial p}{\partial y} + \frac{1}{Re}\Delta v \\ \frac{\partial u}{\partial x} + \frac{\partial v}{\partial y} &= 0 \end{aligned} \tag{1}$$

where $\Delta \equiv \partial^2/\partial x^2 + \partial^2/\partial y^2$ and Re is the Reynolds number, u and v are velocities in x and y-directions and p is the pressure. The set of equations (1) forms a system of three linear partial differential equations in three flow variables (u, v, p). Among these the last equation (continuity equation) has no time derivative. Hence, if algebraic equations are constructed by discretization, the system of equations will be singular.

To overcome this singularity, the velocity-vorticity formulation will be used. Vorticity is defined as $\omega = \nabla \times \overline{u}$, where, $\overline{u}$ is the perturbation in velocity vector; since in the 2D case there is no spanwise variation, the vorticity equation decouples from wall normal velocity and hence may be discarded. Thus, for the 2D case the velocity-vorticity formulation is given as [2],

$$\Delta\dot{v} = \left\{-U\frac{\partial}{\partial x}\Delta + \frac{d^2U}{dy^2}\frac{\partial}{\partial x} + \frac{\Delta^2}{Re}\right\}v \tag{2}$$

with homogeneous boundary conditions

$$v(x, y = \pm 1, t) = 0 \tag{3}$$

$$\frac{\partial v(x, y = \pm 1, t)}{\partial y} = 0 \tag{4}$$

If control inputs are applied at the lower boundary ($y = -1$), this changes the homogenous boundary conditions into non-homogeneous ones. However, the problem can be converted into a non-homogeneous PDE with homogeneous boundary conditions by a change of variables [14]. For this, let us consider,

$$v(x, y, t) = \phi(x, y, t) + q(t)w(x)f(y) \tag{5}$$

where, the function $w(x)$ is a weighting (it represents the effect of control action along x-direction). The function $f(y)$ represents the effect of boundary control on the wall normal velocity profile at location y.

Any function $f(y)$ can be used here provided it fulfills the boundary conditions. However, here we will use the one presented by [4], which is given as,

$$f(y) = \frac{2y^4 + y^3 - 4y^2 - 3y + 4}{4} \tag{6}$$

such that

$$f(-1) = 1, \qquad f(1) = 0, \qquad \left.\frac{df}{dy}\right|_{\pm 1} = 0. \tag{7}$$

In terms of the new variable ϕ the homogeneity in boundary conditions can be recovered. Thus the modified boundary value partial differential equation is given as

$$\begin{aligned} \Delta\dot{\phi} + \dot{q}\Delta(wf) = &-qU\frac{\partial}{\partial x}\Delta(wf) + qf\frac{d^2U}{dy^2}\frac{\partial w}{\partial x} \\ &+q\frac{\Delta^2}{Re}(wf) - U\frac{\partial}{\partial x}\Delta\phi \\ &+\frac{d^2U}{dy^2}\frac{\partial\phi}{\partial x} + \frac{\Delta^2}{Re}\phi \end{aligned} \tag{8}$$

with the Neumann and Dirichlet (ND) boundary conditions given as

$$\phi(x, y = \pm 1, t) = 0, \qquad \frac{\partial\phi(x, y = \pm 1, t)}{\partial y} = 0 \tag{9}$$

III. COMBINED FINITE DIFFERENCE-SPECTRAL MODELING

Equation (8) is a partial differential equation in streamwise (x), wall normal (y) and time (t) variables. In this section we will apply finite difference approximation in x, y-directions. While Chebyshev polynomials will be used to approximate the temporal behavior of the wall normal velocity. The approach is most appropriate for controller synthesis since we have sensors and actuators mounted on the discrete locations at boundaries only.

$$
\begin{aligned}
(S_1+S_1^{-1}-2)\dot{\phi}_i+\frac{\partial^2\dot{\phi}_i}{\partial y^2}+\dot{q}_i\frac{\partial^2 f}{\partial y^2} &= q_i\frac{1}{Re}\frac{\partial^4 f}{\partial y^4}-U(S_1^2-2S_1+2S_1^{-1}-S_1^{-2})\phi_i/2-U(S_1-S_1^{-1})\left(\frac{\partial^2\phi_i}{2\partial y^2}\right)\\
&\quad+\frac{d^2U}{dy^2}(S_1-S_1^{-1})\phi_i/2+\frac{1}{Re}(S_1^2-4S_1-4S_1^{-1}+S_1^{-2}+6)\phi_i\\
&\quad+\frac{2}{Re}(S_1+S_1^{-1}-2)\left(\frac{\partial^2\phi}{\partial y^2}\right)+\frac{1}{Re}\frac{\partial^4\phi_i}{\partial y^4} \qquad (10)
\end{aligned}
$$

$$
\begin{aligned}
\left\{(S_1+S_1^{-1}-2)I_{N+1}\Gamma+\Gamma''\right\}\dot{a}+\dot{q}b_1 &= qb_2-\frac{U}{2}(S_1^2-2S_1+2S_1^{-1}-S_1^{-2})I_{N+1}\Gamma a\\
&\quad-U(S_1-S_1^{-1})I_{N+1}\frac{1}{2}\Gamma'' a+\frac{d^2U}{dy^2}(S_1-S_1^{-1})I_{N+1}\frac{1}{2}\Gamma a\\
&\quad+\frac{1}{Re}(S_1^2-4S_1-4S_1^{-1}+S_1^{-2}+6)\Gamma a\\
&\quad+\frac{2}{Re}(S_1+S_1^{-1}-2)I_{N+1}\Gamma'' a+\frac{1}{Re}\Gamma'''' a \qquad (19)
\end{aligned}
$$

A. Streamwise Discretization

To obtain a finite dimensional approximation of the above PDE, a finite difference scheme is used in streamwise directions. Assuming that the x-direction is discretised into regular spaced samples, one can use a symmetric finite difference approximation of the partial derivatives $\frac{\partial^k}{\partial x^k}$. In this approach we have $w=1$ for each grid point (i) in x-direction. Then introducing the operators S and S^{-1}, which represent a spatial shift to the right and left of the i^{th} grid point, respectively, (8) can be written as (10).

B. Temporal Dynamics

For each grid point (i), in x-direction the time evolution is modeled using a pseudo-spectral approach that was first proposed in [3]. Approximating the free temporal response of the wall normal velocity by truncated Chebyshev polynomials as

$$
\phi_i(t) = \sum_{m=4}^{N} a_m(t)\Gamma_m(y_k) \qquad (11)
$$

Since, the use of ordinary Chebyshev basis functions will not enforce the boundary conditions, these needed to be modified. Here, we will use the modified polynomials defined as [7],

$$
\begin{aligned}
\Gamma_1^M &= \Gamma_1\\
\Gamma_2^M &= \Gamma_2\\
\Gamma_3^M &= \Gamma_3-\Gamma_1\\
\Gamma_4^M &= \Gamma_4-\Gamma_2\\
\Gamma_{m>4,odd}^M &= (\Gamma_m-\Gamma_1)-\frac{(m-1)^2(\Gamma_{m-2}-\Gamma_1)}{(m-3)^2}\\
\Gamma_{m>4,even}^M &= (\Gamma_m-\Gamma_2)-\frac{((m-1)^2-1)(\Gamma_{m-2}-\Gamma_2)}{((m-3)^2-1)} \qquad (12)
\end{aligned}
$$

Then,

$$
\begin{aligned}
\dot{\phi}_i &= \sum_{m=4}^{N}\dot{a_{mi}}(t)\Gamma_m(y_k)\\
\frac{\partial^2\dot{\phi}_i}{\partial y^2} &= \sum_{m=4}^{N}\dot{a_{mi}}(t)\frac{\partial^2\Gamma_m(y_k)}{\partial y^2}\\
\frac{\partial\phi_i}{\partial y} &= \sum_{m=4}^{N}a_{mi}(t)\frac{\partial\Gamma_m(y_k)}{\partial y}\\
\frac{\partial^2\phi_i}{\partial y^2} &= \sum_{m=4}^{N}a_{mi}(t)\frac{\partial^2\Gamma_m(y_k)}{\partial y^2} \qquad (13)
\end{aligned}
$$

$$
\frac{\partial^4\phi_i}{\partial y^4} = \sum_{m=4}^{N}a_{mi}(t)\frac{\partial^4\Gamma_m(y_k)}{\partial y^4} \qquad (14)
$$

C. Wall-normal Direction

To discretize in wall normal-direction, we can make a grid of $N+1$ Chebyshev-Gauss-Lobatto points, y_k, where $y_k=\cos(\pi k/N), \forall\ k=1,...,N$.

Let us now define the following matrices:

$$
a = \begin{bmatrix} a_4 \\ \vdots \\ a_N \end{bmatrix} \qquad (15)
$$

$$
\Gamma = \begin{bmatrix} \Gamma_4(y_2) & \dots & \Gamma_N(y_2) \\ \vdots & \vdots & \vdots \\ \Gamma_4(y_{N-2}) & \dots & \Gamma_N(y_{N-2}) \end{bmatrix} \qquad (16)
$$

$$
\Gamma' = \begin{bmatrix} \frac{\partial\Gamma_4}{\partial y}|_{y_2} & \cdots & \frac{\partial\Gamma_N}{\partial y}|_{y_2} \\ \vdots & \vdots & \vdots \\ \frac{\partial\Gamma_4}{\partial y}|_{y_{N-2}} & \cdots & \frac{\partial\Gamma_N}{\partial y}|_{y_{N-2}} \end{bmatrix} \qquad (17)
$$

$$
b_1 = \begin{bmatrix} \frac{\partial^2 f}{\partial y^2}|_{y_2} \\ \vdots \\ \frac{\partial^2 f}{\partial y^2}|_{y_{N-2}} \end{bmatrix} \quad b_2 = \begin{bmatrix} \frac{1}{Re}\frac{\partial^4 f}{\partial y^4}|_{y_2} \\ \vdots \\ \frac{1}{Re}\frac{\partial^4 f}{\partial y^4}|_{y_N} \end{bmatrix} \qquad (18)
$$

Similarly we define Γ'' and Γ''''. Then, we can write (10) in matrix form as (19). Note that the first four basis functions do not fulfil the ND boundary conditions. This suggests that one should eliminate columns of Γ, Γ', Γ'' and Γ'''' corresponding to these. In order to make the resulting matrices square, one can eliminate the two rows corresponding to the upper and lower walls and the two next to these, as the wall normal velocity near walls must either be zero or very small. Here, the index i is dropped for clarity of notation.

D. Measurement

Let the stream-wise shear stress component at a point in x-direction on the lower wall be given by [5]

$$z_i = \frac{1}{Re}\left(\frac{\partial u}{\partial y} + \frac{\partial v}{\partial x}\right)_{y=-1, x=x_i} \tag{20}$$

Since $\partial v/\partial x$ is known, as it is set by the controller, the measurement vector can be selected as

$$z_i = \frac{1}{Re}\left(\frac{\partial u}{\partial y}\right)_{y=-1, x=x_i} \tag{21}$$

If we subtract the shear stress of two neighboring elements Sx_i and $S^{-1}x_i$, we will get

$$y = 2\frac{(S - S^{-1})}{2Re}\left(\frac{\partial u}{\partial y}\right)_{y=-1} \tag{22}$$

The control system will then look like Figure 2, where G_i and K_i represent flow dynamics and controller at the i^{th} location in x-direction. From the continuity equation we have

$$\frac{\partial^2 u}{\partial x \partial y} = -\frac{\partial^2 v}{\partial y^2} \tag{23}$$

Hence

$$y = -2\frac{1}{Re}\left(\frac{\partial^2 v}{\partial y^2}\right)_{y=-1} \tag{24}$$

Applying change of variables (5) and using (13), we obtain

$$y = -2\frac{1}{Re}\left\{(\mathbf{\Gamma}'')_{(N-2)^{th}row}\mathbf{a} + qw\left(\frac{\partial^2 f}{\partial y^2}\right)_{y=-1}\right\} \tag{25}$$

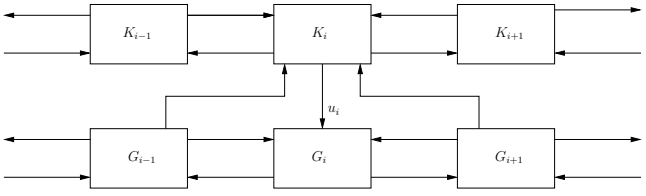

Fig. 2. Flow control system

Then, combining (19) and (25), the linearized dynamics of the flow at the i^{th} grid point in x-direction can be written in state space representation as

$$\begin{bmatrix} \dot{x^t} \\ \mathbf{S}x^s \\ y \end{bmatrix} = \begin{bmatrix} \bar{A}^{tt} & \bar{A}^{ts} & \bar{B}_0^t \\ \bar{A}^{st} & \bar{A}^{ss} & \bar{B}_0^s \\ \bar{C}_0^t & \bar{C}_0^s & \bar{D}_{00} \end{bmatrix} \begin{bmatrix} x^t \\ x^s \\ u \end{bmatrix} \tag{26}$$

where $x^t = \mathbf{a}$, $u = \begin{bmatrix} q^T & \dot{q}^T \end{bmatrix}^T$ and x^s contains the signals which are entering the i^{th} system from left and right. Correspondingly $\mathbf{S}x^s$ are the signals exiting the right and left neighbors.

IV. Discussion

In this section we compare the model constructed here with previously proposed models. The model proposed here has different inputs and outputs, and we will try to give some physical interpretation of the resulting features.

A. Model order

The order of the model is chosen considering two numerical issues: accuracy and conditioning of the resulting matrices. In the spectral approaches, increasing the number of basis functions leads to a more accurate representation of the actual behavior. However, increasing the number of basis functions may make the matrices ill conditioned [7]. Hence, the inversion may lead to considerable numerical errors. Under these considerations the order of the model is chosen as 30.

The model so obtained has a total of 120 states. The model is reduced to 50 states by eliminating states with a small Hankel singular value [15]. It has been observed that this elimination does not produce any significant effect on the system dynamics for low Re and at high Re it still capture the large resonance peak , as shown in Figure 3, where the solid curve shows the frequency response of the full order model.

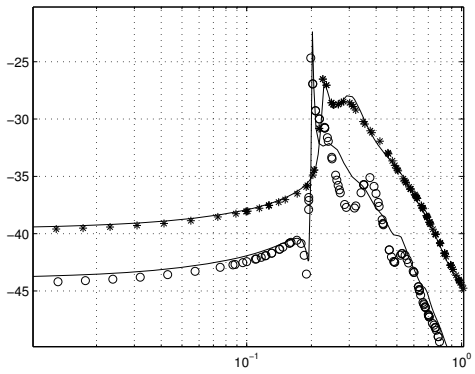

Fig. 3. Maximum singular value plot of flow model at $Re = 10^4$ 'o' and $Re = 5 \times 10^3$ '*'

B. Comparison of model inputs and outputs

The shape of control action for the models which are based on spectral discretization of the streamwise direction is shown in Figure 4.a. The model of [8] has control input as shown in Figure 4.b. These control inputs result in control action where blowing and suction are coupled. Hence, at each time instant the controller generates blowing as well as suction. However, the control input considered here has a general shape as shown in Figure 4.c, which results in either blowing *or* suction at a particular time. Thus, if a disturbance

is applied at the i^{th} point it will effect the complete length of the channel with little delay, compared with the propagation delay in other models. Also, the model output is not the shear force but $\partial F_s/\partial x$, where, F_s is the shear force.

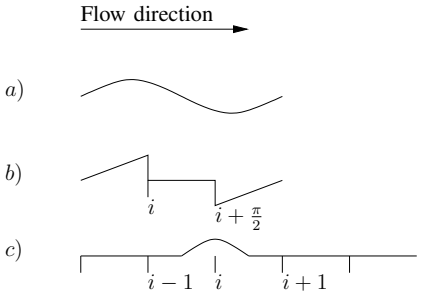

Fig. 4. Control action at the i^{th} node.

C. Comparison with Orr-Sommerfeld equation

The Orr-Sommerfeld equation which governs linear disturbances in 2D parallel flow predicts that at $Re = 10000$ the flow transition occurs in the range $w \approx [0.17, 0.27]$ [8]. This transition from laminar to turbulent flow is generally linked to the presence of an unstable mode which appears in the solution of Orr-Sommerfeld equation for $Re > 5772$. However, it has been pointed out in [16], [17], [5] and [18] that there is no real significance to the unstable mode, as it is not responsible for the transition but it is the transient energy which causes the transition, since the system may invalidate assumptions about linearity. A good measure of transient energy is the $\mathcal{L}_2$-norm of the transfer function from disturbance to output [1]. Thus, for large Reynolds numbers the $\mathcal{L}_2$-norm must get larger to predict the transition.

It can be seen in Figure 3 that the input to output gain grows in a band of $w = [0.17, 0.27]$, with a large resonant peak at 0.2 and 0.23 rad/sec for $Re = 10^4$ and 5000, respectively. Which is the same as predicted by Orr-Sommerfeld. However, no unstable mode is observed for $R_e > 5772$. However, the $\mathcal{L}_2$-norm gets larger, as can be seen in Figure 3, which predicts the transition due to poorly damped oscillations.

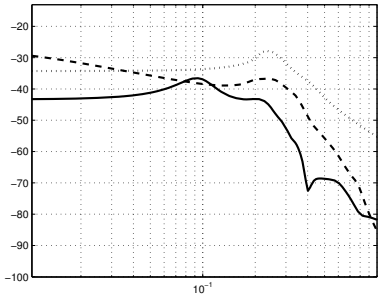

Fig. 5. Gain of the system for disturbance applied at i^{th} node and change in shear force 2 (dotted), 5 (dashed), 10 (solid) units upstream for $Re = 2000$

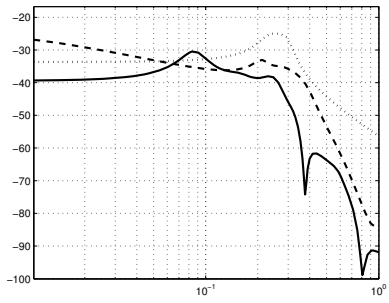

Fig. 6. Gain of the system for disturbance applied at i^{th} node and change in shear force 2 (dotted), 5 (dashed), 10 (solid) units downstream for $Re = 2000$

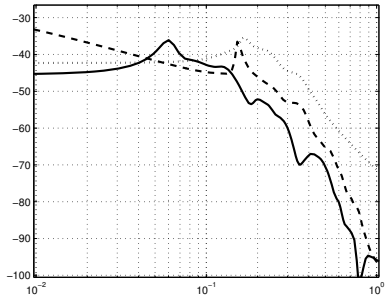

Fig. 7. Gain of the system for disturbance applied at i^{th} node and change in shear force 2 (dotted), 5 (dashed), 10 (solid) units upstream for $Re = 10000$

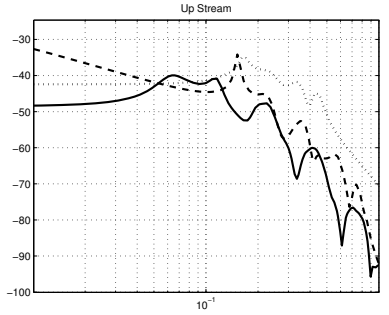

Fig. 8. Gain of the system for disturbance applied at i^{th} node and change in shear force 2 (dotted), 5 (dashed), 10 (solid) units downstream for $Re = 10000$

D. Spatial stability

To further analyze the spatial behavior of the system, the frequency response between a disturbance applied at the i^{th} unit and the change in shear force $[2, 5, 10]$ units downstream and upstream are obtained for $Re = [2000, 10000]$. These responses are shown in Figure 5, Figure 6, Figure 7 and Figure 8. It can be observed in these figures that for large Re the disturbance can generate poorly damped oscillations both upstream and downstream, thus causing spatial instability.

Further more, the effect of disturbance is nearly similar both upstream and downstream. This behavior is due to the particular shape of disturbance (as shown in Figure 4.c.) chosen for this model. While a low value of the gain is

attributed to the fact that the output chosen is not shear force but its spatial change, as explained earlier.

V. Controller Synthesis

In order to demonstrate the usage of the proposed model for designing a controller in physical domain, we designed a dynamic full order (order equal to the order of the plant) output feedback controller based on the approach of [10].

For brevity let us define $x^T = \begin{bmatrix} x^{t^T} & x^{s^T} \end{bmatrix}$. Using the approach of [10] it can be shown that if a system has state space representation (26), the closed loop system is stable if the following inequality holds:

$$\bar{A_{cl}}^T X_{cl} + X_{cl} \bar{A_{cl}} < 0 \tag{27}$$

where $\bar{A_{cl}}$ is the A-matrix of the closed loop system, $(\bar{A_{cl}})$ refers to the application of a bilinear transformation to the discretized spatial part and $X_{cl} = diag(X^t, X^s)$. Here X^t is a symmetric positive definite matrix, and X^s is a symmetric matrix. Using the double sided projection lemma on (27) we obtain the following set of LMIs in a reduced number of decision variables

$$\begin{aligned} NR'(\bar{A}^T R + R\bar{A})NR < 0 \\ NQ'(Q\bar{A}^T + \bar{A}Q)NQ < 0 \\ \begin{bmatrix} R^t & I \\ I & Q^t \end{bmatrix} < 0 \end{aligned} \tag{28}$$

where NR and NS are matrices whose columns span the null space of $\bar{B}^T$ and $\bar{C}$, respectively, and $R = diag(R^t, R^s)$ and $Q = diag(Q^t, Q^s)$ are block diagonal symmetric matrices. Once a feasible solution to these LMIs is found the controller matrices can be constructed using the approach given in [10].

The approach is applied to the flow transition model obtained in section 3 for a Reynold number of 6000. Using the above LMIs, a stabilizing controller is synthesized for this case, thus achieving spatial stability. The controller so obtained can be used in interconnected form for an infinite length of channel as shown in Figure 2, where $K_i = K_{i+1} = K_{i-1}$.

VI. Conclusions

In this paper a new model for plane Poiseuille flow is presented. The model is based on a combined spectral-finite difference approach. The velocity-vorticity formulation of the NSE equations is used. It has been demonstrated that the model predicts the dominating features of the plane Poiseuille flow. This suggests that it can therefore be used for synthesizing a controller to control the transition from laminar to turbulent flow. As a first step towards controller synthesis, a stabilizing full order dynamic output feedback controller is designed.

Since finite difference approaches approximate the pseudo spectra of a non-normal operator better than the spectral approaches, as discussed in [19] and [20], it is expected that the model presented here can lead to better controllers than those based on spectral models. A detailed investigation and comparison of the pseudo spectra of both models is the subject of current work. Another topic of future work is to use the proposed model for the synthesis of low-order and fixed-structure controllers, based on the approach presented in [11].

References

[1] T. Bewley, "Flow control: new challenges for a new renaissance," *Progress in Aerospace sciences*, vol. 37, no. 1, pp. 21–58, 2001.

[2] R. Peyret, *Spectral methods for incompressible viscous flow*, Applied Mathematical Science. Springer, Berlin, 2002.

[3] S. Orszag, "Accurate solution of the Orr-Sommerfeld stability equation," *Journal of Fluid Mechanics*, vol. 50, no. 4, pp. 689–703, 1971.

[4] S. Joshi, J. Speyer, and J. Kim, "A system theory approach to the feedback stabilization of infinitesimal and finite-amplitude disturbances in plane Poiseuille flow," *Journal of Fluid Mechanics*, vol. 332, pp. 157–184, 1997.

[5] T. Bewley and S. Liu, "Optimal and robust control and estimation of linear paths to transition," *Journal of Fluid Mechanics*, vol. 365, no. 12, pp. 305–349, 1998.

[6] M. Hogberg, T. Bewley, and D. Henningson, "Linear feedback control and estimation of transition in plane channel flow," *Journal of Fluid Mechanics*, vol. 481, pp. 149–175, 2003.

[7] J. McKernan, *Control of plane Poiseuille flow: A theoretical and computational investigation*, Ph.D. thesis, Cranfield University, Dept. of Aerospace Siences, School of Engineering, 2006.

[8] L. Baramov, O. Tutty, and E. Rogers, "H_∞ control of nonperiodic two-dimensional channel flow," *IEEE Transactions on Control Systems Technology*, vol. 12, no. 1, pp. 111–122, 2004.

[9] O. Daube, "Resolution of the 2D Navier-Stokes equations in velocity-vorticity forms by means of an influence matrix technique," *Journal of Computational Physics*, vol. 103, pp. 402–414, 1992.

[10] R. D'Andrea and G. E. Dullerud, "Distributed control design for spatially interconnected systems," *IEEE Transactions on Automatic Control*, vol. 48, no. 9, pp. 1478–1495, 2003.

[11] S. S. Chughtai and H. Werner, "Fixed structure controller design for a class of spatially interconnected systems," in *Proceedings IFAC Symposium on Large Scale Systems*, 2007.

[12] S. S. Chughtai and H. Werner, "Distributed control for a class of spatially interconnected discrete-time systems," in *Proc. IFAC World Congress 2008*, 2008, pp. 7761–7766.

[13] S. S. Chughtai and H. Werner, "New dilated lmis to synthesize controllers for a class of spatially interconnected systems," in *Proc. IFAC World Congress 2008*, 2008, pp. 7767–7771.

[14] J. Boyd, *Chebyshev and Fourier Spectral Methods*, Dover Publications Inc., NewYork, 2001.

[15] S. Skogestad and I. Postlethwaite, *Multivariable Feedback Control - Analysis and Design*, John Wiley & Sons, Ltd., 2005.

[16] K. Butler and B. Farrell, "Three dimensional optimal disturbances in viscous shear flow," *Physics of Fluids*, vol. 4, no. 8, pp. 1637–1650, 1992.

[17] L. Trefethen, A. Trefethen, S. Reddy, and T. Driscoll, "Hydrodynamic stability without eigenvalues," *Science*, vol. 261, no. 30, pp. 578–584, 1993.

[18] M. Jovanovic and B. Bamieh, "Unstable modes versus non-normal modes in supercritical channel flows," in *Proc. American Control Conference*, Boston, Massachusetts, USA, 2004.

[19] A. Harrabi, "On the approximation of pseudospectra of non normal operators by discretization, part 1: the first derivative operator," Tech. Rep., CERFACS, 1998.

[20] A. Harrabi, "On the approximation of pseudospectra of non normal operators by discretization, part 2: The convection-diffusion operator," Tech. Rep., CERFACS, 1998.